

Physics of the heliosphere: an introduction

Lectures at the „Escuela Mexicana de Astrofísica 2002“
July 31 to Aug 7, 2002
by Rainer Schwenn, MPAe Lindau

3. Solar wind and corona in 3D

- Stream boundaries and interactions
- The 3D heliosphere at activity minimum
- Puzzles at high latitudes
- A new understanding of heliospheric rotation
- The two states of the solar wind

2002/08/05 10:20

Remember: how to measure the solar wind

The principle of electrostatic analyzers

Spherical deflection plates with an applied voltage let charged particles pass if their energy/charge fits:
 $E/q = m/2 * V^2/q = U \cdot 1/d \cdot R$

Detectors at the exit of the plates count the successful particles.

Quadrupole plates with several detectors allow determination of one angle of incidence.

Rotation of the detector, e.g. on a spinning spacecraft, allows determination of the other angle of incidence.

The voltage is stepped through and the successful particles per step are counted.

The way the particle fluxes of all energy/charge values at all angles of incidence can be measured and a 3D velocity distribution function can be derived.

Proton 3D velocity distributions for various wind speeds and distances from the sun as measured by Helios

The closer to the sun and the higher the wind speed, the higher the density!

By integration over $f(v) v^n d^3v$ one gets the „moments“ of the distribution function:

- $n=0$ number density n
- $n=1$ bulk velocity v
- $n=2$ temperature T
- $n=3$ heat flux

This calculation works „precisely“ only in case of Maxwellian distributions. In other cases, e.g., the solar wind, non-Maxwellian parts of the distribution functions are lost!

Two types of solar wind: evidence from Helios

The stream fronts are steeper closer to the Sun a surprise for some modelers...

Helios plasma measurements during first approach to perihelion (0.3 AU).

Two different types of solar wind!

1. Fast wind in high speed streams

- High speed: 400-800 kms⁻¹
- Low density: 3 cm⁻³
- Low particle flux: 2×10^8 cm⁻² s⁻¹
- Helium content: 3.6%, stationary
- Source: coronal holes
- Signatures: stationary for long times, all streams are alike, strong Alfvénic fluctuations.

2. Low speed wind of "interstream" type

- Low speed: 250-400 kms⁻¹
- High density: 10.7 cm⁻³
- High particle flux: 3.7×10^8 cm⁻² s⁻¹
- Helium content: below 2%, highly variable
- Source: helmet streamers near current sheet, at activity minimum
- Signatures: generally very variable, sector boundaries imbedded.

The Parker spiral and the formation of Corotating Interaction Regions (CIRs)

The "Parker spiral". The curvature depends strongly on the solar wind speed:
 $\tan \alpha = \Omega R / v$

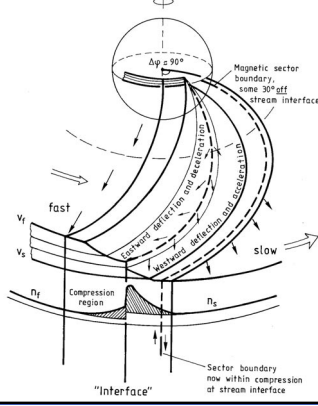
In case fast wind follows slow wind, a Corotating Interaction Region (CIR) forms, where the plasma is compressed and deflected.

Stream interfaces at high speed stream fronts

Longitudinal speed gradients of high speed stream fronts, as measured by Helios between 0.3 and 1 AU.

The closer to the sun, the steeper the fronts!

Scheme of the radial evolution of a CIR



The originally sharp front separating streams of different speed widens because of stream-stream interactions. By about 1 AU all solar wind has been "processed" this way.

That marks the border between "inner" and "outer" heliosphere.

From stream interface to CIR and shock pair

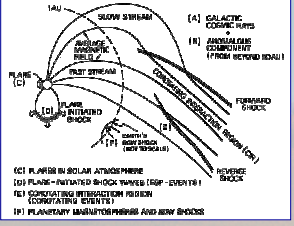
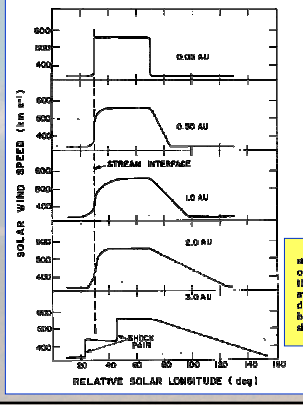
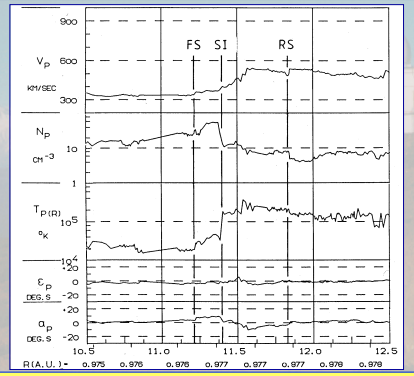


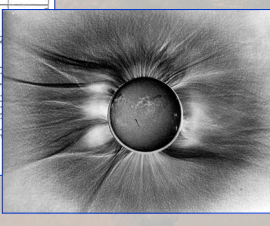
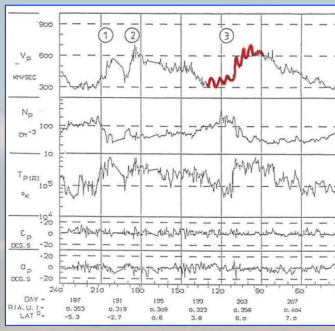
Fig. 10. The evolution of an idealized high-speed solar wind stream with increasing heliocentric distances. Observations at the orbit of the earth (1 AU) indicate that the edges of many streams close to the sun contain large velocity shears. Solar rotation induces an asymmetric evolution of the edges of the idealized streams with increasing distance from the sun, the shear at the westmost edge of the stream becoming the stream interface. In the visible white light corona these shears might be identified as the outer edges of coronal streamers.

From stream interface to CIR and shock pair



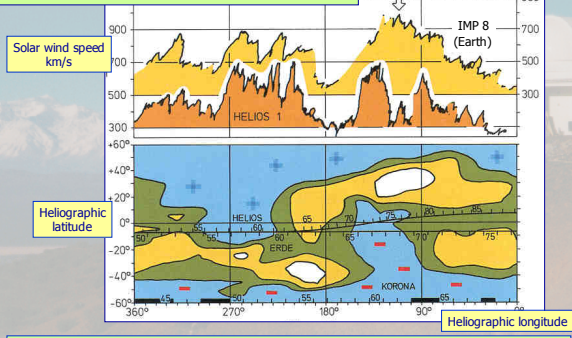
A stream interface with a TD and a corotating shock pair, observed by Helios even inside 1 AU

The filamentary structure of the solar wind



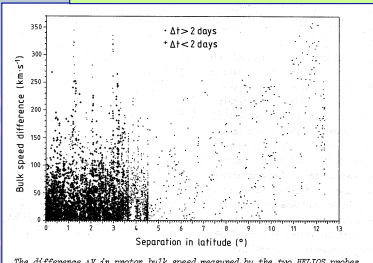
The angular size of the solar wind tube is ~5°. It corresponds well to the scale size of the expanded polar plume structure known from eclipses.

Latitudinal stream boundaries



Solar wind stream structure, seen nearly simultaneously from 1 AU and from 0.3 AU (IMP and Helios 1) in early 1975, associated with coronal hole structure. Note that Helios passed the northern boundary of the fast stream, while IMP at low latitude did not.

Latitudinal stream boundaries



This was our 1976 argument for the solar wind being a two-state-phenomenon!

The difference Δt in proton bulk speed measured by the two HELIOS probes as a function of their separation in heliographic latitude $\Delta\lambda$. Each point represents an average over 2° in solar longitude. The crosses denote cases with observation times of less than two days.

Summarizing our observations of "leading", "trailing" and "latitudinal" boundaries, we conclude that fast streams near 0.3 AU exhibit sharp boundaries in all directions. This finding, taken together with the observation of mesa-like profiles of large fast streams near 0.3 AU, implies that possibly because of new critical points developing in highly diverging flows (Kopp and Holzer, 1976), solar wind emerges from the corona in two different states, a "fast" and a "slow" one. This idea will be followed up in section 5.3 of this paper.

The two states of corona and solar wind

Active regions and streamers let the „slow wind“ emerge

Coronal holes produce the „fast wind“

The corona of sun at beginning activity (1998), viewed by EIT and LASCO-C1/C2

LASCO C1/C2, on 1.2. 1996

The corona at activity minimum in early 1996 and its topology:

- there are magnetic multipole structures at mid-latitudes, in addition to the general dipole,
- these helmets may involve multiple current sheets,
- the mid latitude loops appear to be very stable in time, i.e., they extend over substantial longitudes as do the underlying photospheric neutral lines,
- the near-equatorial helmets vary strongly and are often absent.

The streamer sheet (only 30 deg wide in interplanetary space!) and the HCS imbedded in it are products of the mid-latitude streamers close to the sun, NOT of the activity belt near the equator!

LASCO C1/C2, on 1.2. 1996

slow wind

fast wind

Coronal hole Boundary

streamer sheet

HCS

streamer belt

The corona at activity minimum in early 1996 and its topology.

The equatorial streamer belt

The boundaries of coronal holes and the streamer belt, as seen by EIT and UVCS on SOHO

Note that the streamer belt close to the sun is about one solar diameter wide. That had already been inferred from several minimum eclipses.

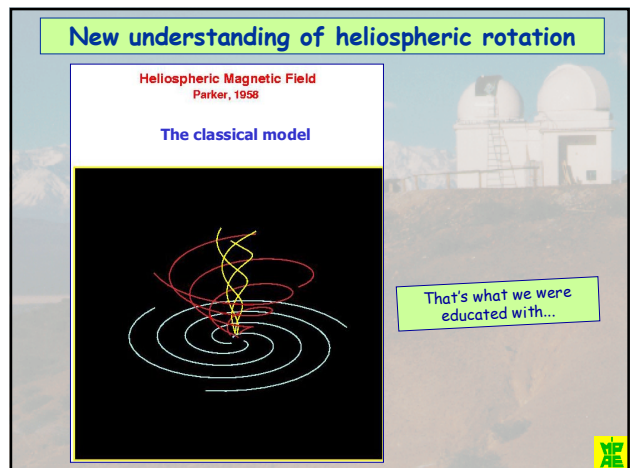
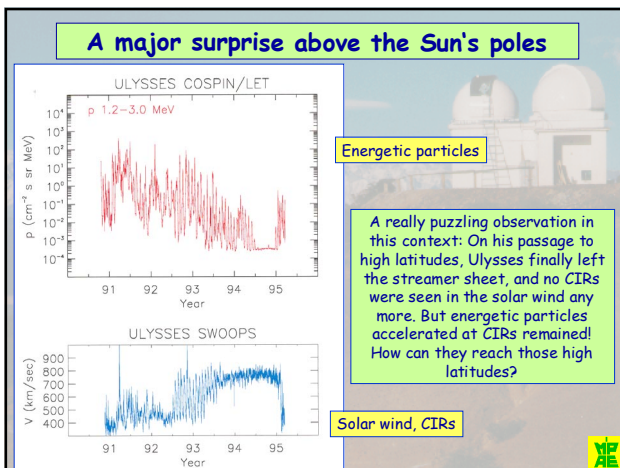
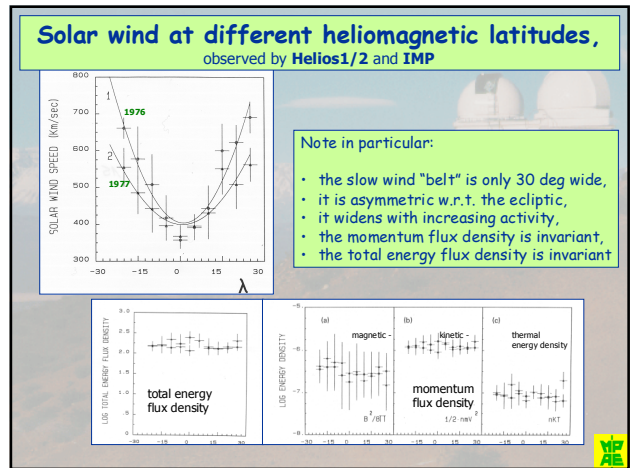
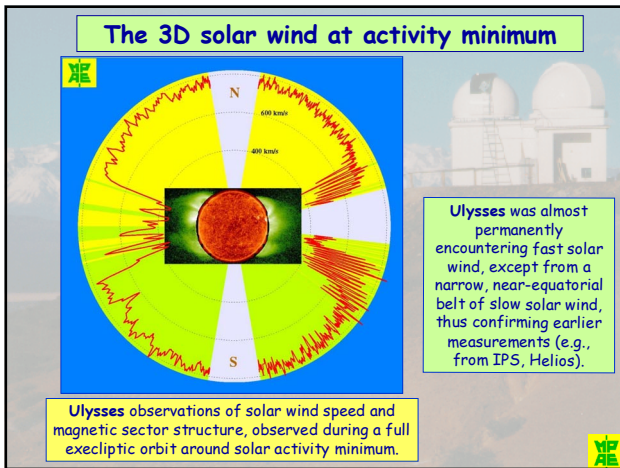
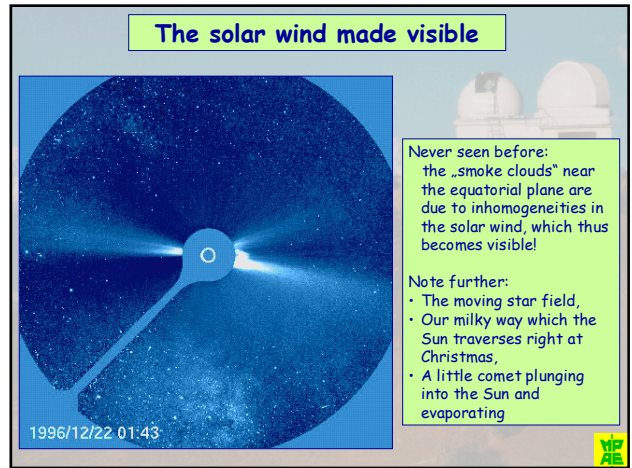
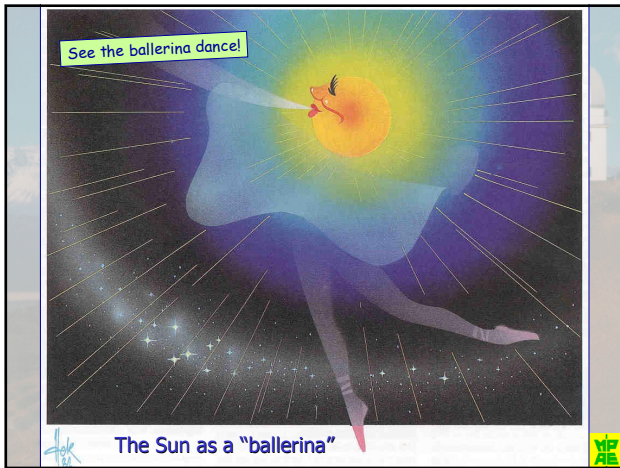
See the ballerina dance!

The Sun as a "ballerina", according to Alfvén, 1977.

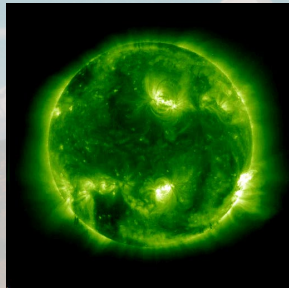
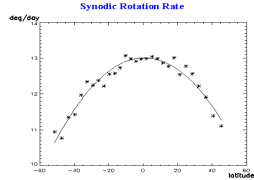
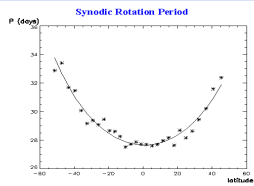
See the ballerina dance!

1996-08-11 23:02 UT

The Sun and its corona at solar activity minimum during the Whole Sun Month (WSM) in 1996, seen by the LASCO C1/C2 coronagraphs on SOHO and the WSO magnetograph



New understanding of heliospheric rotation

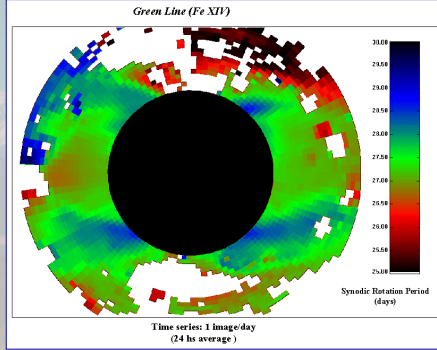


The short term motion of coronal patterns occurs accurately according to differential rotation

as determined from EIT FeXII Images (1-14 April 1997) by determining the longitude displacement of the pattern after a given time interval



New understanding of heliospheric rotation



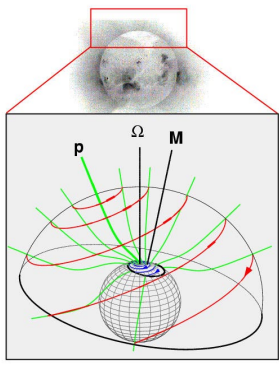
Rotation periods of corotating coronal features, determined from LASCO-C1 data

However, long-lived coronal patterns exhibit a uniform rotation of the whole corona at the equatorial rotation period (27.2 days).



New understanding of heliospheric rotation

Coronal Magnetic Field at High Latitude:

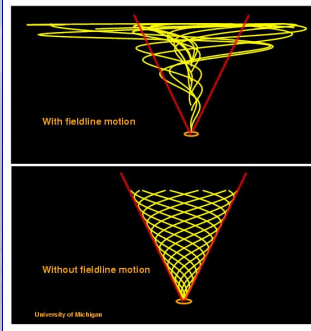


The new "Fisk" model. It involves differential rotation, the inclined solar axis and reconnection.



New understanding of heliospheric rotation

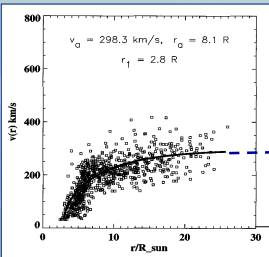
Heliospheric Magnetic Field Fisk, 1996



In this scheme, field lines emerging at high latitudes can reach down to low latitudes, where energetic particles might be injected.

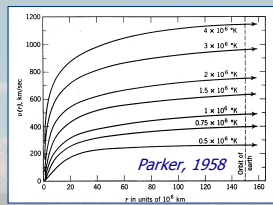


The „slow“ solar wind, at low latitudes



Speed profiles of the slow solar wind, as determined from „leaves in the wind“

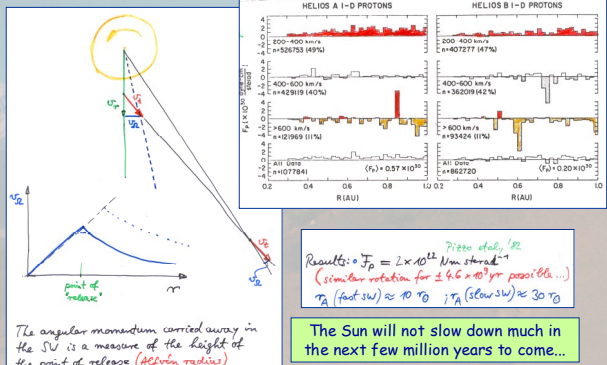
Note: coherent outward flow starts only at about 3 R_s the profile is consistent with in-situ speed profiles obtained by Helios between 60 and 210 R_s



Helios at 60 R_s

60

The solar wind carries away angular momentum



The Sun will not slow down much in the next few million years to come...



The „fast“ wind: full of Alfvén waves

Helium ions, surfing on Alfvén waves

Sie machen die Wellenbewegung nicht mit!

in machen die Wellenbewegung mit!

auswärtiges gerichtetes Magnetfeld

einwärts gerichtetes Magnetfeld

Alfvén waves and surfing α -particles...

The „fast“ wind: full of Alfvén waves

Alfvén waves cause substantial deflections in both: flow direction and magnetic field.

That is the origin of strong north-south field excursions in high speed wind streams

The „fast“ wind: full of Alfvén waves

Alfvén waves in high speed streams cause magnetic excursions including southward B_z -components which cause moderate geomagnetic effects!

High speed streams: M-regions!

Often ignored: High speed streams from coronal holes (i.e. the inactive" sun) cause (moderate) geomagnetic activity: **They are the "M-regions"!** They are most prominent in the years right before activity minima. Then, the polar coronal holes may have large extensions reaching to equatorial latitudes such that the high speed streams appear in the ecliptic plane as well.

The "musical diagram" of geomagnetic activity, according to the scheme introduced by Bartels (1930)

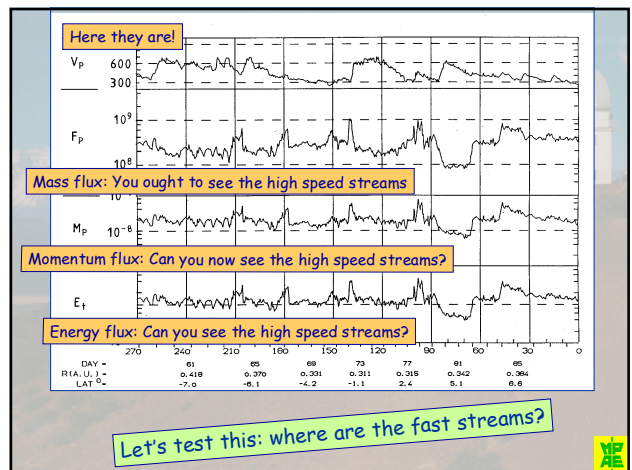
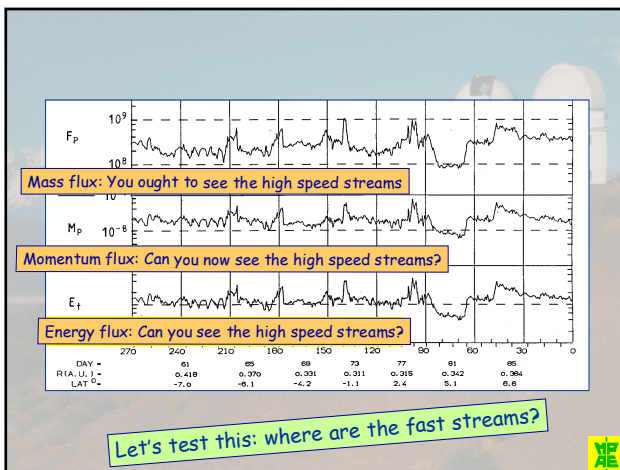
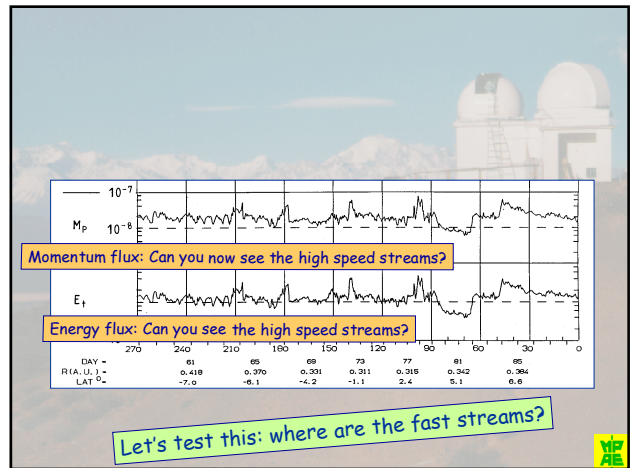
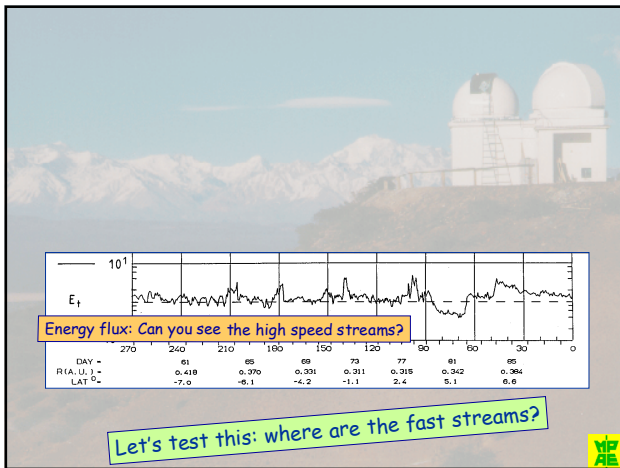
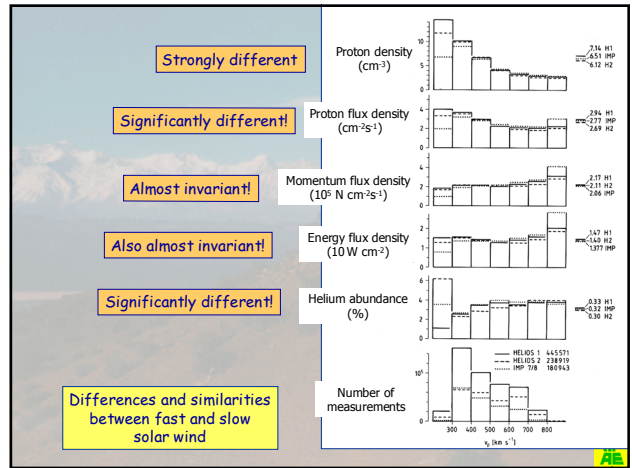
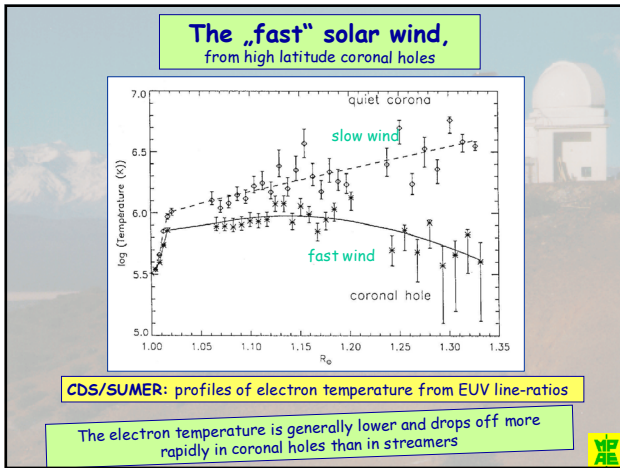
The „fast“ solar wind, from high latitude coronal holes

The SOHO instruments have shown, that the fast solar wind from coronal holes emerges from the network boundaries, in particular from their intersections

The „fast“ solar wind, from high latitude coronal holes

UVCS on SOHO measured the proton and O^{5+} ion thermal speeds in a coronal hole. For reference, the electron thermal speeds are shown as well.

Note the pronounced preferential heating and acceleration of Oxygen with respect to the protons, thus indicating ion cyclotron heating, at least in case of the fast solar wind



The two basic states of the solar wind

Differences	slow wind	fast wind
Speed		faster
Density	higher	
Helium content	lower, variable	constant 3.6%
Nature	transient	„quiet“ wind
Angular momentum	almost all	almost none
Sources	above active regions	coronal holes
Source temperature	hot	cold
Acceleration onset	$> 3R_{\odot}$	close to surface
Acceleration done	$> 10R_{\odot}$	$3R_{\odot}$
Ion cyclotron heating	no evidence	strong evidence
$V_{\alpha} > V_{\beta}$	no	yes
Alfvén waves	none	much
FIP effect	strong	none

Similarities momentum flux density
total energy flux density

Apparently, there are two basic types of solar wind, resulting from different acceleration mechanisms



Where the heliosphere ends

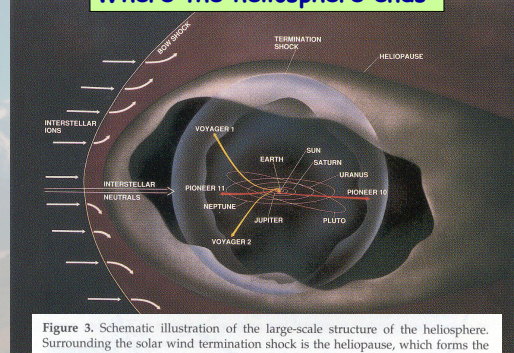
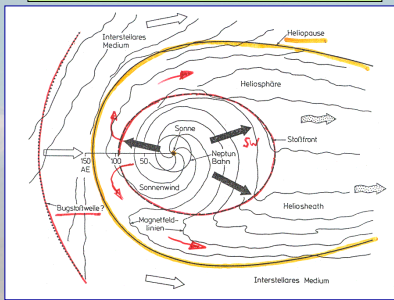


Figure 3. Schematic illustration of the large-scale structure of the heliosphere. Surrounding the solar wind termination shock is the heliopause, which forms the interface between solar and interstellar plasma, and a possible "bow shock" that may be located beyond the heliopause. The present positions of the Pioneer and Voyager spacecraft are indicated. The termination shock is assumed to be 67 AU from the Sun, as derived from an analysis of 1987 anomalous cosmic ray data from Pioneer 10 and Voyager 2.



Where the heliosphere ends



Local interstellar medium (LISM):
 B_{α} : 0.3 to 0.5 nT
 T_i : 10^4 K
 V_i : 27 km s⁻¹
 N_i : 0.1 cm⁻³

Solar wind (at 1 AU)
 B_{sw} : 2 nT
 T_{sw} : 10^5 K
 V_{sw} : 400 km s⁻¹
 N_{sw} : 5 cm⁻³



Where the heliosphere ends

$$P_s = P_B + P_T + P_U + P_{CR}$$

$$\frac{n_E m v_E^2}{R^2 \cdot K} = \alpha \cdot \frac{B_i^2}{8\pi} + 2n_i kT_i + n_i m v_i^2 + P_{CR}$$

mit $K = 1.15$ (Korrektur HP \rightarrow TS)
 $\alpha = 2.25$ ("draping" des IS Magnetfeldes)

[dyn cm⁻²] $\sim 10^{-12}$ \uparrow 10^{-15} \uparrow 10^{-15} \uparrow ?

$\sim R_s$ also $R_s(B_i; n_i)$
 Anford.

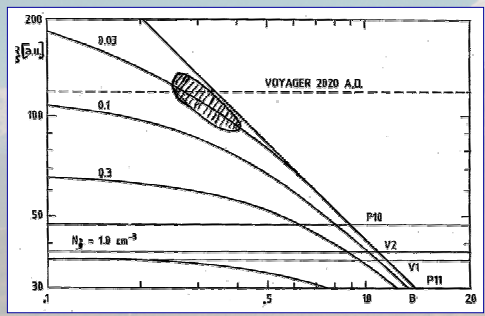
This simple estimate gives the distance R_s of the heliospheric termination shock as function of the properties of the interstellar plasma B_i, T_i, n_i . The main unknowns are the effective pressure of the GCRs and the potential effects of the interstellar neutral gas.

This approach has been successfully used to estimate the stand-off distance of the Earth's bow shock

Pressure equilibrium at the heliopause



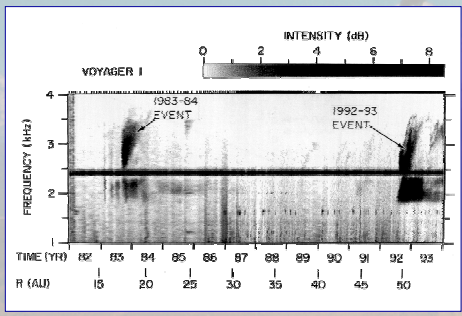
Where the heliosphere ends



With the given assumptions, the size of the heliosphere can be estimated from this graph

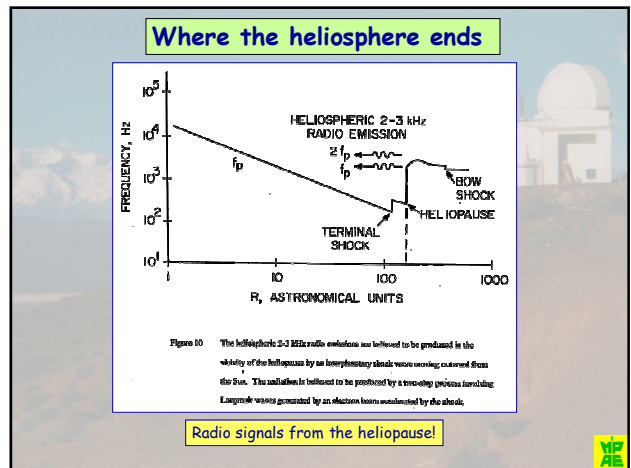
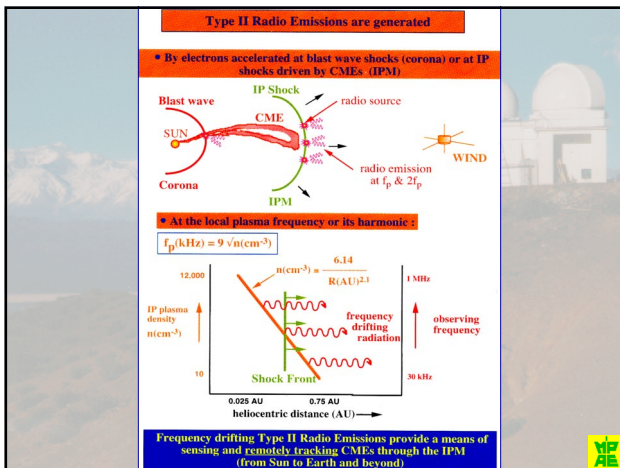


Where the heliosphere ends



Radio signals from the heliopause!





Basic questions about the solar wind still waiting to be answered

- How is the corona being heated?
- How is the slow wind released?
- What heats and accelerates the fast wind?
- Why these sharp boundaries?
- Spatial scales of the crucial physical processes?
- Differential rotation, rigid rotation, "Fisk effect"?
- Solar wind dropouts and other strange escapades?
- Abundance variations and FIP effect?
- Where does the heliosphere end?
- ?
- ?

Physics of the heliosphere: an introduction

Lectures at the
„Escuela Mexicana de Astrofísica 2002“
July 31 to August 7, 2002
by Rainer Schwenn, MPAe Lindau

3. Solar wind and corona in 3D

- Stream boundaries and interactions
- The 3D heliosphere at activity minimum
- Puzzles at high latitudes
- A new understanding of heliospheric rotation
- The two states of the solar wind